

0.1 Results: ΛK_S^0 and ΛK^\pm

In the following sections, we present results assuming (i) no residual correlations (Sec. 0.1.3), (ii) three residual contributors (Sec. 0.1.1), and (iii) ten residual contributors (Sec. 0.1.2). We find the case of three and ten contributors to be consistent; therefore, for simplicity, we will quote the result utilizing three residuals as our final result.

For the results shown, unless otherwise noted, the following hold true: All correlation functions were normalized in the range $0.32 < k^* < 0.40$ GeV/c, and fit in the range $0.0 < k^* < 0.30$ GeV/c. For the ΛK^- and $\bar{\Lambda} K^+$ analyses, the region $0.19 < k^* < 0.23$ GeV/c was excluded from the fit to exclude the bump caused by the Ω^- resonance. The non-femtoscopic background was modeled by a (6th)-order polynomial fit to THERMINATOR simulation. The $\Lambda K^+(\bar{\Lambda} K^-)$ radii are shared with $\Lambda K^-(\bar{\Lambda} K^+)$, while the $\Lambda K_S^0(\bar{\Lambda} K_S^0)$ radii are unique. In the figures showing experimental correlation functions with fits, the black solid line represents the primary (ΛK) correlation's contribution to the fit. The green line shows the fit to the non-flat background. The purple points show the fit after all residuals' contributions have been included, and momentum resolution and non-flat background corrections have been applied.

Before beginning, I first collect a summary of my final results in Figure 1. In the summary plot, we show the extracted scattering parameters in the form of a $\text{Im}[f_0]$ vs $\text{Re}[f_0]$ plot, which includes the d_0 values to the right side. We also show the λ vs. radius parameters for all three of our studied centrality bins. In Fig. 1, three residual contributors were used, and the background was modeled by a (6th)-order polynomial fit to THERMINATOR simulation. For the ΛK_S^0 results shown in the figure, the ΛK_S^0 and $\bar{\Lambda} K_S^0$ analyses were fit simultaneously across all centralities (0-10%, 10-30%, 30-50%); scattering parameters and a single λ parameter were shared amongst all, the radii were shared amongst results of like-centrality, and each has a unique normalization parameter. For the ΛK^\pm results shown, all four pair combinations were fit simultaneously (ΛK^+ , $\bar{\Lambda} K^-$, ΛK^- , $\bar{\Lambda} K^+$) across all centralities. Scattering parameters were shared between pair-conjugate systems (i.e. a parameter set describing ΛK^+ & $\bar{\Lambda} K^-$, and a separate set describing ΛK^- & $\bar{\Lambda} K^+$). For each centrality, a radius and λ parameters were shared between all pairs. Each analysis has a unique normalization parameter.

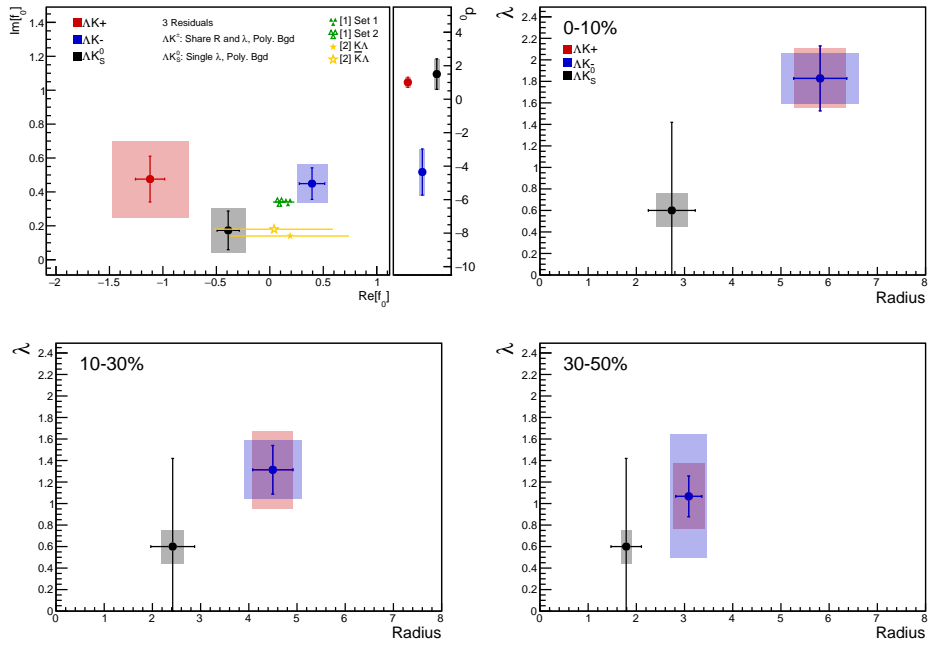


Fig. 1: Extracted scattering parameters for the case of 3 residual contributors for all of our AK systems. [Top Left]: $\text{Im}[f_0]$ vs. $\text{Re}[f_0]$, together with d_0 to the right. [Top Right (Bottom Left, Bottom Right)]: λ vs. Radius for the 0-10% (10-30%, 30-50%) bin. The green [?] and yellow [?] points show theoretical predictions made using chiral perturbation theory.

0.1.1 3 Residual Correlations Included in Fit

Figure 2 nicely collects and summarizes all of our extracted fit parameters for the case of 3 included residual contributors. Figure 3 presents our extracted fit radii, along with those of other systems previously analyzed by ALICE [?], as a function of pair transverse mass (m_T). Figures 4, 5, and 6 show the experimental correlation functions with fits, assuming 3 residual contributors, for all studied centralities for ΛK_S^0 with $\bar{\Lambda} K_S^0$, ΛK^+ with $\bar{\Lambda} K^-$, and ΛK^- with $\bar{\Lambda} K^+$, respectively. The parameter sets extracted from the fits can be found in Tables 5 and 6.

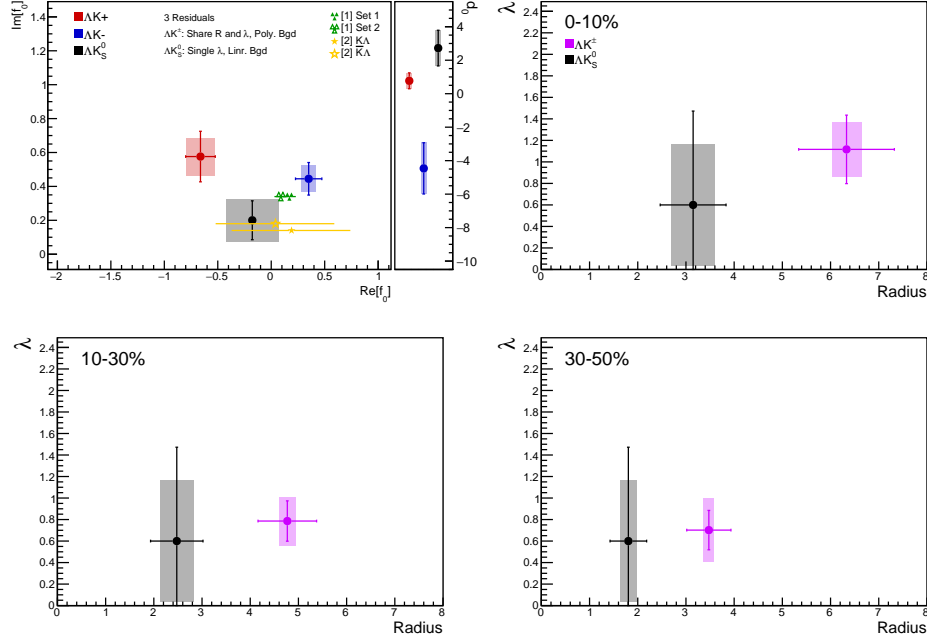


Fig. 2: Extracted scattering parameters for the case of 3 residual contributors for all of our ΛK systems. [Top Left]: $\text{Im}f_0$ vs. $\text{Re}f_0$, together with d_0 to the right. [Top Right (Bottom Left, Bottom Right)]: λ vs. Radius for the 0-10% (10-30%, 30-50%) bin. The green [?] and yellow [?] points show theoretical predictions made using chiral perturbation theory.

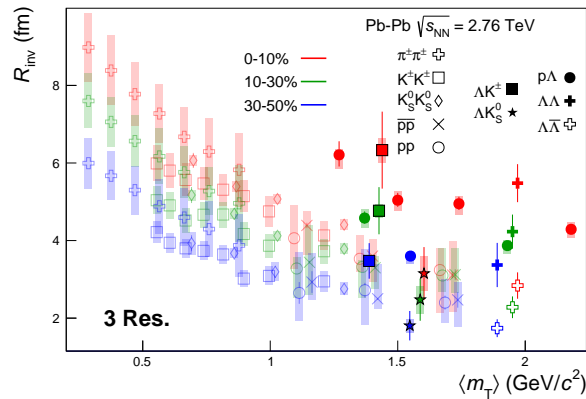
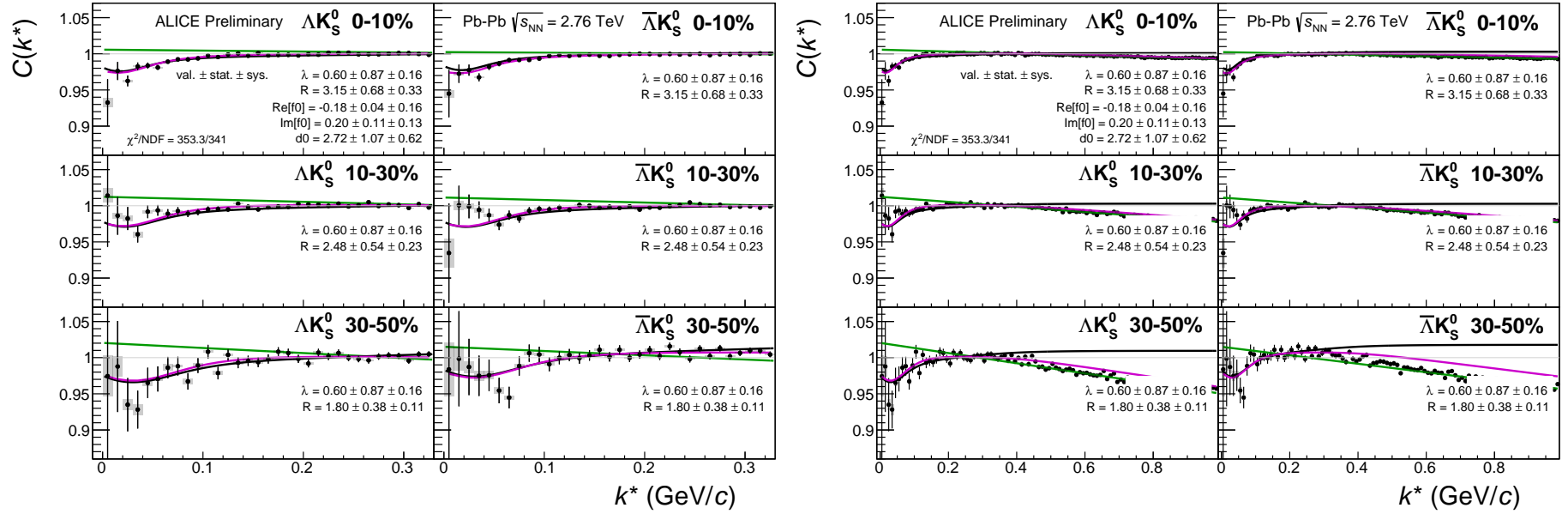


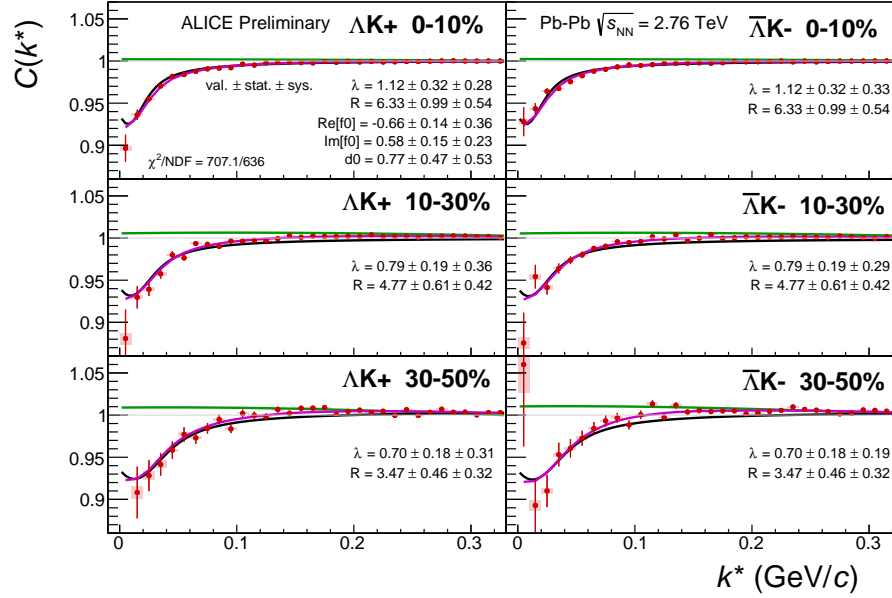
Fig. 3: 3 residual correlations in ΛK fits. Extracted fit R_{inv} parameters as a function of pair transverse mass (m_T) for various pair systems over several centralities. The ALICE published data [?] is shown with transparent, open symbols. The new ΛK results are shown with opaque, filled symbols. In the left, the ΛK^+ (with it's conjugate pair) results are shown separately from the ΛK^- (with it's conjugate pair) results. In the right, all ΛK^\pm results are averaged.



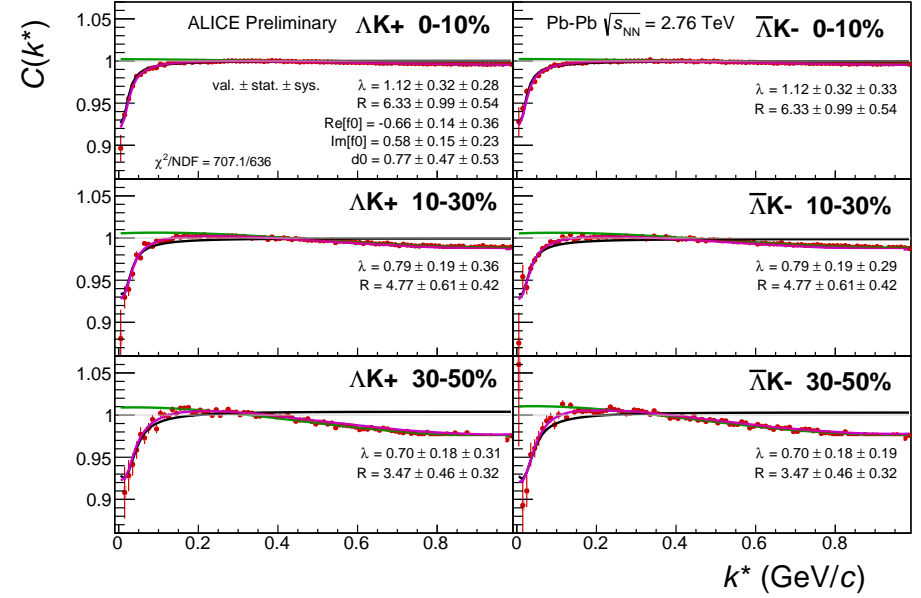
(a) Signal region view ($k^* \lesssim 0.3$ GeV/c)

(b) Wide view ($k^* \lesssim 1.0$ GeV/c)

Fig. 4: Fits, with 3 residual correlations included, to the ΛK_S^0 (left) and $\bar{\Lambda} K_S^0$ (right) data for the centralities 0-10% (top), 10-30% (middle), and 30-50% (bottom). The lines represent the statistical errors, while the boxes represent the systematic errors. A single λ parameter is shared amongst all. Each analysis has a unique normalization parameter. The radii are shared between analyses of like centrality, as these should have similar source sizes. The scattering parameters ($\text{Re}[f_0]$, $\text{Im}[f_0]$, d_0) are shared amongst all. The background is modeled by a (6th-)degree polynomial fit to THERMINATOR simulation. The black solid line represents the primary (ΛK) correlation's contribution to the fit. The green line shows the fit to the non-flat background. The purple points show the fit after all residuals' contributions have been included, and momentum resolution and non-flat background corrections have been applied. The extracted fit values with uncertainties are printed.

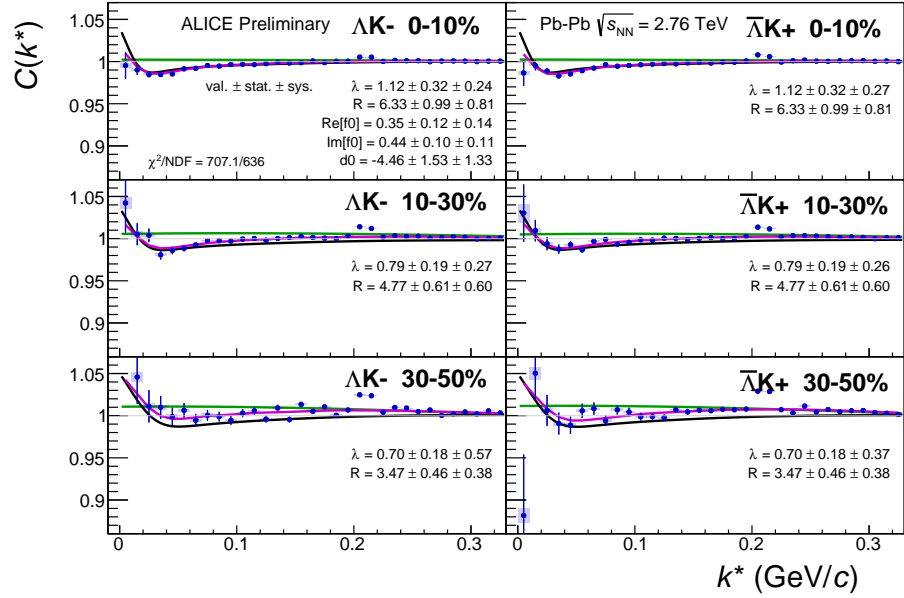


(a) Signal region view ($k^* \lesssim 0.3$ GeV/c)

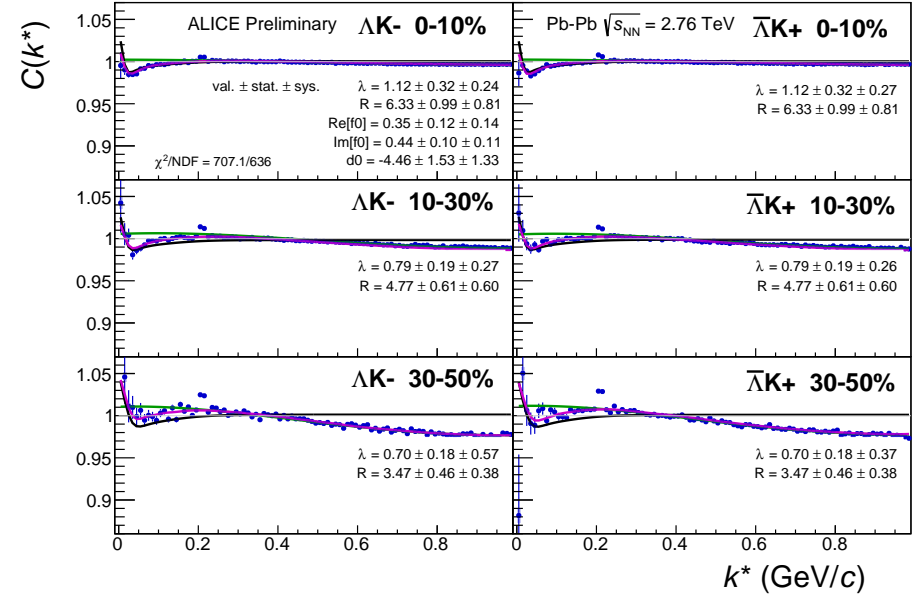


(b) Wide view ($k^* \lesssim 1.0$ GeV/c)

Fig. 5: Fits, with 3 residual correlations included, to the ΛK^+ (left) and $\bar{\Lambda} K^-$ (right) data for the centralities 0-10% (top), 10-30% (middle), and 30-50% (bottom). The lines represent the statistical errors, while the boxes represent the systematic errors. All ΛK^\pm analyses are fit simultaneously across all centralities (0-10%, 10-30%, 30-50%). Scattering parameters ($\text{Re} f_0$, $\text{Im} f_0$, d_0) are shared between pair-conjugate systems (i.e. a parameter set describing the ΛK^+ & $\bar{\Lambda} K^-$ system, and a separate set describing the ΛK^- & $\bar{\Lambda} K^+$ system). For each centrality, a radius and λ parameters are shared between all pairs (ΛK^+ , $\bar{\Lambda} K^-$, ΛK^- , $\bar{\Lambda} K^+$). Each analysis has a unique normalization parameter. The background is modeled by a (6th-)degree polynomial fit to THERMINATOR simulation. The black solid line represents the primary (ΛK) correlation's contribution to the fit. The green line shows the fit to the non-flat background. The purple points show the fit after all residuals' contributions have been included, and momentum resolution and non-flat background corrections have been applied. The extracted fit values with uncertainties are printed.



(a) Signal region view ($k^* \lesssim 0.3$ GeV/c)



(b) Wide view ($k^* \lesssim 1.0$ GeV/c)

Fig. 6: Fits, with 3 residual correlations included, to the ΛK^- (left) with $\bar{\Lambda} K^+$ (right) data for the centralities 0-10% (top), 10-30% (middle), and 30-50% (bottom). The lines represent the statistical errors, while the boxes represent the systematic errors. All ΛK^\pm analyses are fit simultaneously across all centralities (0-10%, 10-30%, 30-50%). Scattering parameters ($\Re f_0$, $\Im f_0$, d_0) are shared between pair-conjugate systems (i.e. a parameter set describing the ΛK^+ & $\bar{\Lambda} K^-$ system, and a separate set describing the ΛK^- & $\bar{\Lambda} K^+$ system). For each centrality, a radius and λ parameters are shared between all pairs (ΛK^+ , $\bar{\Lambda} K^-$, ΛK^- , $\bar{\Lambda} K^+$). Each analysis has a unique normalization parameter. The background is modeled by a (6th-)degree polynomial fit to THERMINATOR simulation. The black solid line represents the “raw” fit, i.e. not corrected for momentum resolution effects nor non-flat background. The green line shows the fit to the non-flat background. The purple points show the fit after momentum resolution and non-flat background corrections have been applied. The extracted fit values with uncertainties are printed.

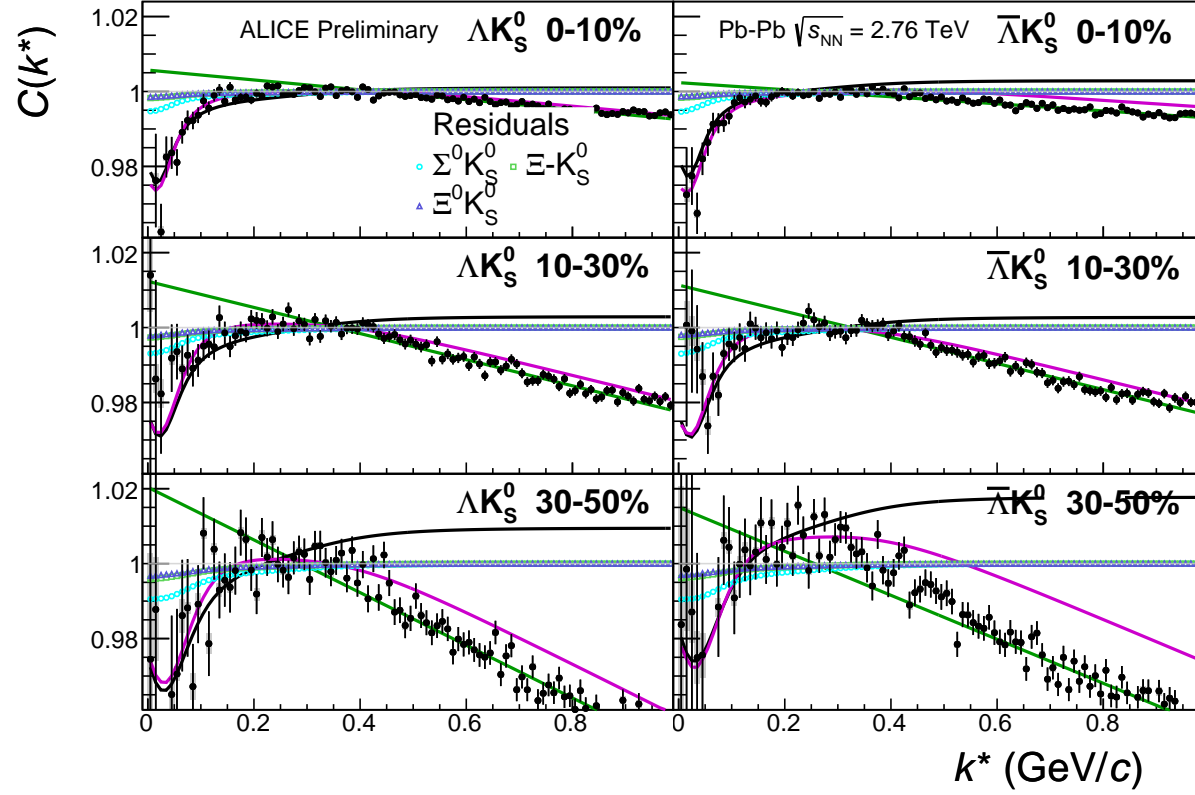
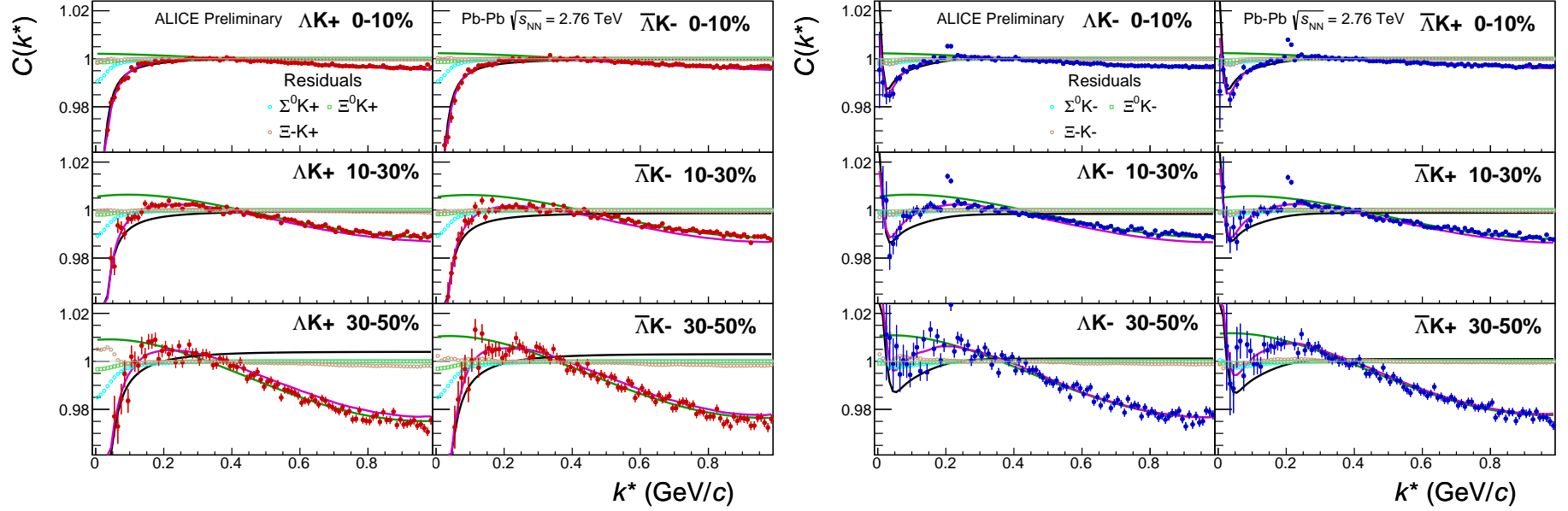


Fig. 7: Fits, with 3 residual correlations included and shown, to the ΛK_S^0 (left) and $\bar{\Lambda} K_S^0$ (right) data for the centralities 0-10% (top), 10-30% (middle), and 30-50% (bottom). The three parent pairs used for the residual correction to the ΛK_S^0 ($\bar{\Lambda} K_S^0$) fit are $\Sigma^0 K_S^0$, $\Xi^- K_S^0$, and $\Xi^0 K_S^0$ ($\bar{\Sigma}^0 K_S^0$, $\bar{\Xi}^- K_S^0$, and $\bar{\Xi}^0 K_S^0$).



(a) $\Lambda K^+(\bar{\Lambda} K^-)$ fits with residual contributions shown for the centralities 0-10% (top), 10-30% (middle), and 30-50% (bottom)

(b) $\Lambda K^-(\bar{\Lambda} K^+)$ fits with residual contributions shown for the centralities 0-10% (top), 10-30% (middle), and 30-50% (bottom)

Fig. 8: Fits, with 3 residual correlations included and shown, to the ΛK^+ & $\bar{\Lambda} K^-$ (left) and ΛK^- & $\bar{\Lambda} K^+$ (right) data for the centralities 0-10% (top), 10-30% (middle), and 30-50% (bottom). The three parent pairs used for the residual correction to the ΛK^+ ($\bar{\Lambda} K^-$) fit are $\Sigma^0 K^+$, $\Xi^0 K^+$, and $\Xi^- K^+$ ($\bar{\Sigma}^0 K^-$, $\bar{\Xi}^0 K^-$, and $\bar{\Xi}^+ K^-$).

Fit Results $\Lambda(\bar{\Lambda})K_S^0$						
System	Centrality	Fit Parameters				
		λ	R	$\Re f_0$	$\Im f_0$	d_0
ΛK_S^0 & $\bar{\Lambda} K_S^0$	0-10%		3.15 ± 0.68 (stat.) ± 0.45 (sys.)			
	10-30%	0.60 ± 0.87 (stat.) ± 0.57 (sys.)	2.48 ± 0.54 (stat.) ± 0.35 (sys.)	-0.18 ± 0.04 (stat.) ± 0.25 (sys.)	0.20 ± 0.11 (stat.) ± 0.13 (sys.)	2.72 ± 1.07 (stat.) ± 2.12 (sys.)
	30-50%		1.80 ± 0.38 (stat.) ± 0.17 (sys.)			

Table 1: Fit Results $\Lambda(\bar{\Lambda})K_S^0$, with 3 residual correlations included. Each pair is fit simultaneously with its conjugate (ie. ΛK_S^0 with $\bar{\Lambda} K_S^0$) across all centralities (0-10%, 10-30%, 30-50%), for a total of 6 simultaneous analyses in the fit. A single λ parameter is shared amongst all. Each analysis has a unique normalization parameter. The radii are shared between analyses of like centrality, as these should have similar source sizes. The scattering parameters ($\Re f_0$, $\Im f_0$, d_0) are shared amongst all. The background is fit with a linear form in the range $0.6 < k^* < 0.9$ GeV/c. The fit is done on the data with only statistical error bars. The errors marked as “stat.” are those returned by MINUIT. The errors marked as “sys.” are those which result from my systematic analysis (as outlined in Section ??).

Fit Results $\Lambda(\bar{\Lambda})K^\pm$						
System	Centrality	Fit Parameters				
		λ	R	$\Re f_0$	$\Im f_0$	d_0
ΛK^+ & $\bar{\Lambda} K^-$	0-10%	1.12 ± 0.32 (stat.) ± 0.25 (sys.)	6.33 ± 0.99 (stat.) ± 0.31 (sys.)	-0.66 ± 0.14 (stat.) ± 0.13 (sys.)	0.58 ± 0.15 (stat.) ± 0.11 (sys.)	0.77 ± 0.47 (stat.) ± 1.66 (sys.)
	10-30%	0.79 ± 0.19 (stat.) ± 0.23 (sys.)	4.77 ± 0.61 (stat.) ± 0.17 (sys.)			
ΛK^- & $\bar{\Lambda} K^+$	30-50%	0.70 ± 0.18 (stat.) ± 0.30 (sys.)	3.47 ± 0.46 (stat.) ± 0.10 (sys.)	0.35 ± 0.12 (stat.) ± 0.07 (sys.)	0.44 ± 0.10 (stat.) ± 0.08 (sys.)	-4.46 ± 1.53 (stat.) ± 1.36 (sys.)

Table 2: Fit Results $\Lambda(\bar{\Lambda})K^\pm$, with 3 residual correlations included. All ΛK^\pm analyses are fit simultaneously across all centralities (0-10%, 10-30%, 30-50%). Scattering parameters ($\Re f_0$, $\Im f_0$, d_0) are shared between pair-conjugate systems (i.e. a parameter set describing the ΛK^+ & $\bar{\Lambda} K^-$ system, and a separate set describing the ΛK^- & $\bar{\Lambda} K^+$ system). For each centrality, a radius and λ parameters are shared between all pairs (ΛK^+ , $\bar{\Lambda} K^-$, ΛK^- , $\bar{\Lambda} K^+$). Each analysis has a unique normalization parameter. The background is modeled by a (6th)-degree polynomial fit to THERMINATOR simulation. The fit is done on the data with only statistical error bars. The errors marked as “stat.” are those returned by MINUIT. The errors marked as “sys.” are those which result from my systematic analysis (as outlined in Section ??).

0.1.2 10 Residual Correlations Included in Fit

Figure 9 nicely collects and summarizes all of our extracted fit parameters for the case of 10 included residual contributors. Figure 10 presents our extracted fit radii, along with those of other systems previously analyzed by ALICE [?], as a function of pair transverse mass (m_T). Figures 11, 12, and 13 show the experimental correlation functions with fits, assuming 10 residual contributors, for all studied centralities for ΛK_S^0 with $\bar{\Lambda} K_S^0$, ΛK^+ with $\bar{\Lambda} K^-$, and ΛK^- with $\bar{\Lambda} K^+$, respectively. The parameter sets extracted from the fits can be found in Tables ?? and ??.

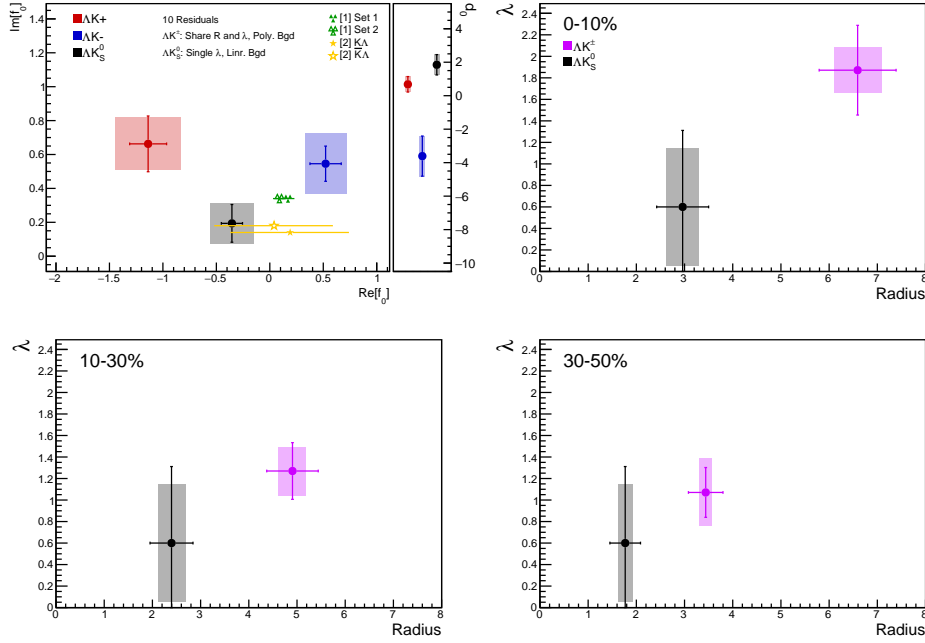


Fig. 9: Extracted scattering parameters for the case of 10 residual contributors for all of our ΛK systems. [Top Left]: $\Im f_0$ vs. $\Re f_0$, together with d_0 to the right. [Top Right (Bottom Left, Bottom Right)]: λ vs. Radius for the 0-10% (10-30%, 30-50%) bin. The green [?] and yellow [?] points show theoretical predictions made using chiral perturbation theory.

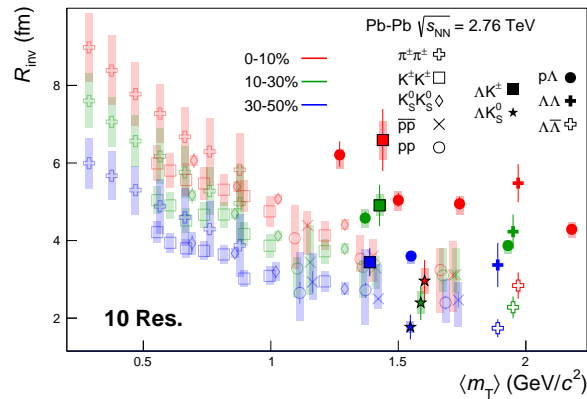
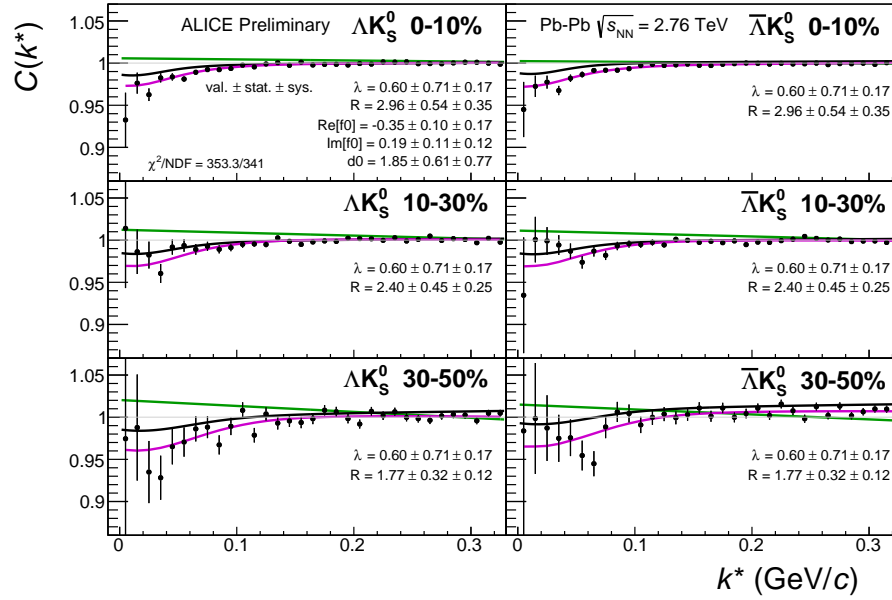
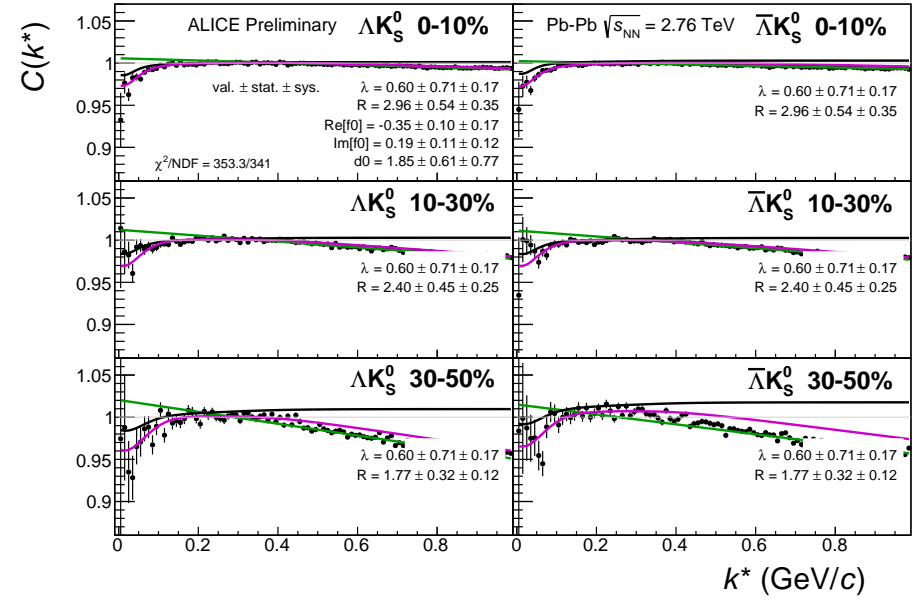


Fig. 10: 10 residual correlations in ΛK fits. Extracted fit R_{inv} parameters as a function of pair transverse mass (m_T) for various pair systems over several centralities. The ALICE published data [?] is shown with transparent, open symbols. The new ΛK results are shown with opaque, filled symbols. In the left, the ΛK^+ (with it's conjugate pair) results are shown separately from the ΛK^- (with it's conjugate pair) results. In the right, all ΛK^\pm results are averaged.

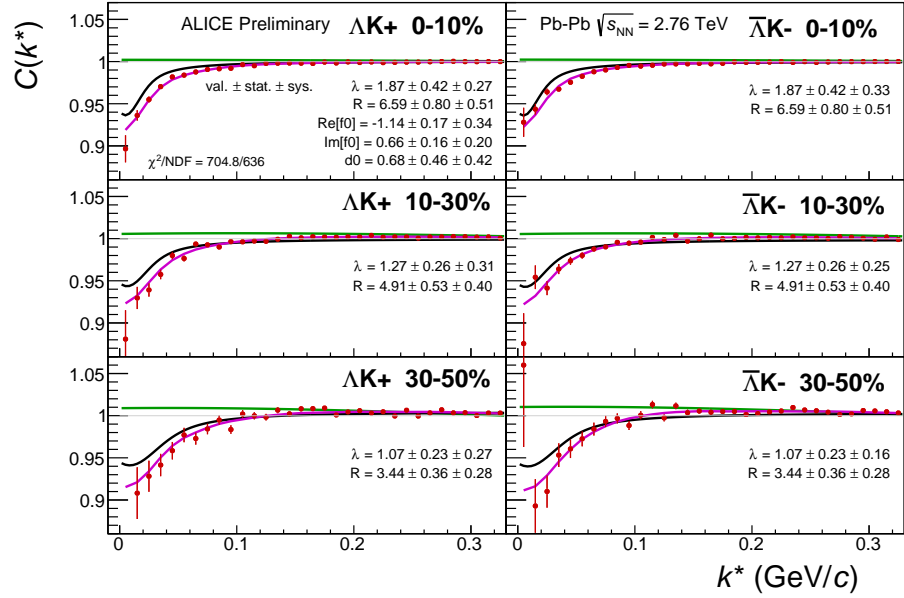


(a) Signal region view ($k^* \lesssim 0.3$ GeV/c)

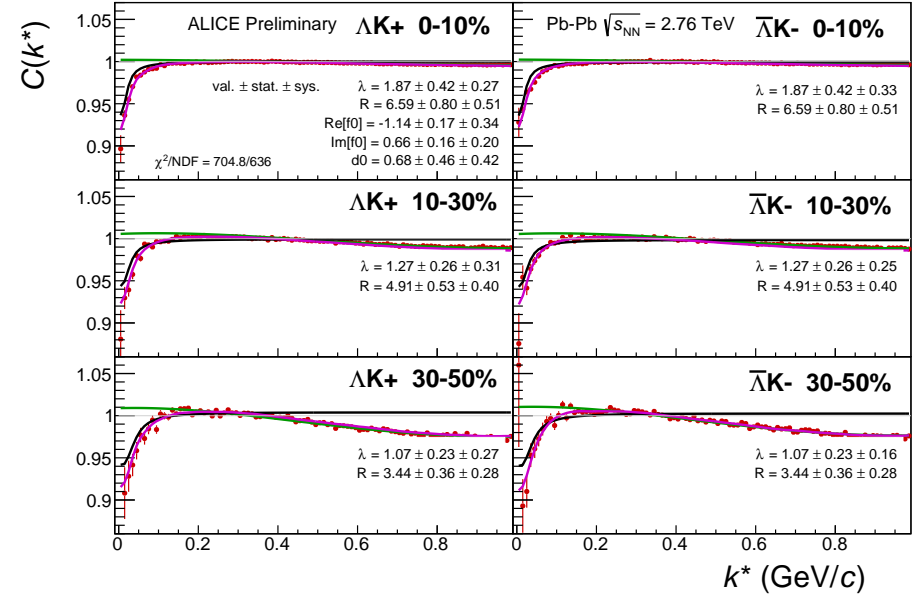


(b) Wide view ($k^* \lesssim 1.0$ GeV/c)

Fig. 11: Fits, with 10 residual correlations included, to the ΛK_S^0 (left) and $\bar{\Lambda} K_S^0$ (right) data for the centralities 0-10% (top), 10-30% (middle), and 30-50% (bottom). The lines represent the statistical errors, while the boxes represent the systematic errors. A single λ parameter is shared amongst all. Each analysis has a unique normalization parameter. The radii are shared between analyses of like centrality, as these should have similar source sizes. The scattering parameters ($\text{Re}[f_0]$, $\text{Im}[f_0]$, d_0) are shared amongst all. The background is modeled by a (6th-)degree polynomial fit to THERMINATOR simulation. The black solid line represents the primary (ΛK) correlation's contribution to the fit. The green line shows the fit to the non-flat background. The purple points show the fit after all residuals' contributions have been included, and momentum resolution and non-flat background corrections have been applied. The extracted fit values with uncertainties are printed.

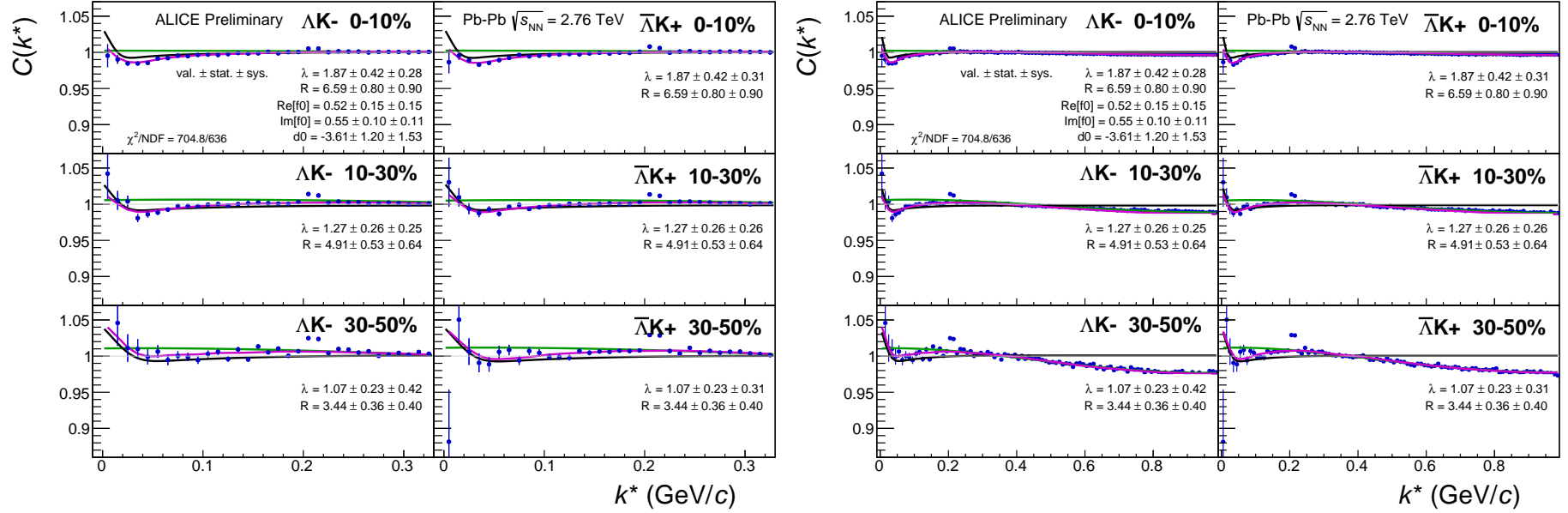


(a) Signal region view ($k^* \lesssim 0.3$ GeV/c)



(b) Wide view ($k^* \lesssim 1.0$ GeV/c)

Fig. 12: Fits, with 10 residual correlations included, to the ΛK^+ (left) and $\bar{\Lambda} K^-$ (right) data for the centralities 0-10% (top), 10-30% (middle), and 30-50% (bottom). The lines represent the statistical errors, while the boxes represent the systematic errors. All ΛK^\pm analyses are fit simultaneously across all centralities (0-10%, 10-30%, 30-50%). Scattering parameters ($\Re f_0$, $\Im f_0$, d_0) are shared between pair-conjugate systems (i.e. a parameter set describing the ΛK^+ & $\bar{\Lambda} K^-$ system, and a separate set describing the ΛK^- & $\bar{\Lambda} K^+$ system). For each centrality, a radius and λ parameters are shared between all pairs (ΛK^+ , $\bar{\Lambda} K^-$, ΛK^- , $\bar{\Lambda} K^+$). Each analysis has a unique normalization parameter. The background is modeled by a (6th-)degree polynomial fit to THERMINATOR simulation. The black solid line represents the primary (ΛK) correlation's contribution to the fit. The green line shows the fit to the non-flat background. The purple points show the fit after all residuals' contributions have been included, and momentum resolution and non-flat background corrections have been applied. The extracted fit values with uncertainties are printed.



(a) Signal region view ($k^* \lesssim 0.3$ GeV/c)

(b) Wide view ($k^* \lesssim 1.0$ GeV/c)

Fig. 13: Fits, with 10 residual correlations included, to the ΛK^- (left) with $\bar{\Lambda} K^+$ (right) data for the centralities 0-10% (top), 10-30% (middle), and 30-50% (bottom). The lines represent the statistical errors, while the boxes represent the systematic errors. All ΛK^\pm analyses are fit simultaneously across all centralities (0-10%, 10-30%, 30-50%). Scattering parameters ($\text{Re}f_0$, $\text{Im}f_0$, d_0) are shared between pair-conjugate systems (i.e. a parameter set describing the ΛK^+ & $\bar{\Lambda} K^-$ system, and a separate set describing the ΛK^- & $\bar{\Lambda} K^+$ system). For each centrality, a radius and λ parameters are shared between all pairs (ΛK^+ , $\bar{\Lambda} K^-$, ΛK^- , $\bar{\Lambda} K^+$). Each analysis has a unique normalization parameter. The background is modeled by a (6th-)degree polynomial fit to THERMINATOR simulation. The black solid line represents the primary (ΛK) correlation's contribution to the fit. The green line shows the fit to the non-flat background. The purple points show the fit after all residuals' contributions have been included, and momentum resolution and non-flat background corrections have been applied. The extracted fit values with uncertainties are printed.

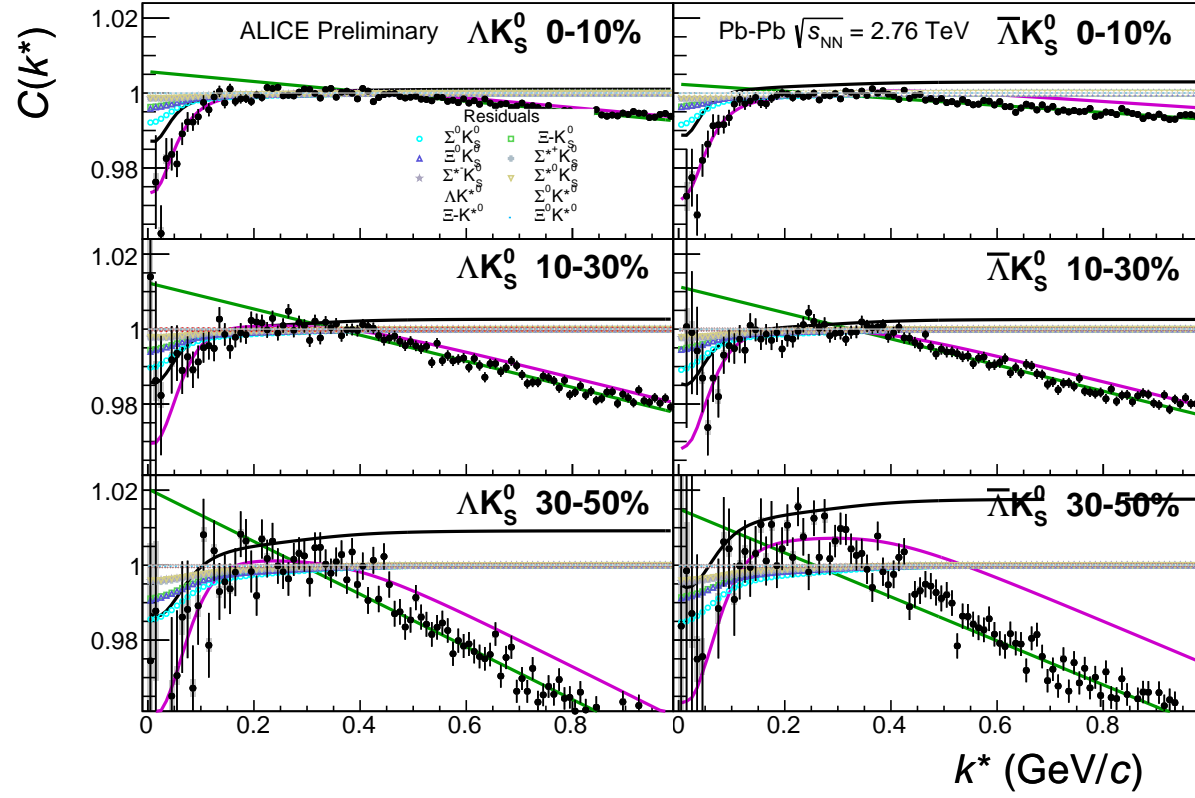
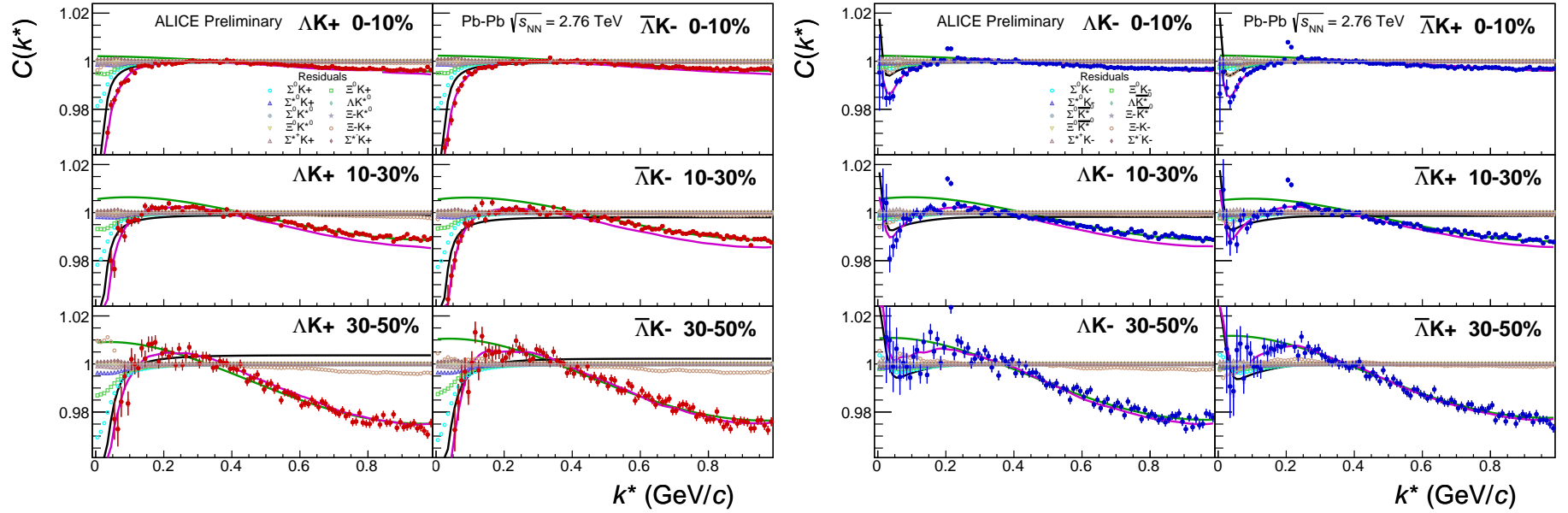


Fig. 14: Fits, with 10 residual correlations included and shown, to the ΛK_S^0 (left) and $\bar{\Lambda} K_S^0$ (right) data for the centralities 0-10% (top), 10-30% (middle), and 30-50% (bottom). The ten parent pairs used for the residual correction to the ΛK_S^0 ($\bar{\Lambda} K_S^0$) fit are $\Sigma^0 K_S^0$, $\Xi^0 K_S^0$, $\Xi^- K_S^0$, $\Sigma^{*0} K_S^0$, ΛK^{*0} , $\Sigma^0 K^{*0}$, $\Xi^0 K^{*0}$, and $\Xi^- K^{*0}$ ($\bar{\Sigma}^0 K_S^0$, $\bar{\Xi}^0 K_S^0$, $\bar{\Xi}^- K_S^0$, $\bar{\Sigma}^{*0} K_S^0$, $\bar{\Lambda} K^{*0}$, $\bar{\Sigma}^0 K^{*0}$, $\bar{\Xi}^0 K^{*0}$, and $\bar{\Xi}^- K^{*0}$).



(a) ΛK^+ ($\bar{\Lambda} K^-$) fits with residual contributions shown for the centralities 0-10% (top), 10-30% (middle), and 30-50% (bottom)

(b) ΛK^- ($\bar{\Lambda} K^+$) fits with residual contributions shown for the centralities 0-10% (top), 10-30% (middle), and 30-50% (bottom)

Fig. 15: Fits, with 10 residual correlations included and shown, to the ΛK^+ & $\bar{\Lambda} K^-$ (left) and ΛK^- & $\bar{\Lambda} K^+$ (right) data for the centralities 0-10% (top), 10-30% (middle), and 30-50% (bottom). The ten parent pairs used for the residual correction to the ΛK^+ ($\bar{\Lambda} K^-$) fit are $\Sigma^0 K^+$, $\Xi^0 K^+$, $\Xi^- K^+$, $\Sigma^{*(+, -, 0)} K^+$, ΛK^{*0} , $\Sigma^0 K^{*0}$, $\Xi^0 K^{*0}$, and $\Xi^- K^{*0}$ ($\bar{\Sigma}^0 K^-$, $\bar{\Xi}^0 K^-$, $\bar{\Xi}^+ K^-$, $\bar{\Sigma}^{*(+, -, 0)} K^-$, $\bar{\Lambda} K^{*0}$, $\bar{\Sigma}^0 K^{*0}$, $\bar{\Xi}^0 K^{*0}$, and $\bar{\Xi}^+ K^{*0}$).

Fit Results $\Lambda(\bar{\Lambda})K_S^0$						
System	Centrality	Fit Parameters				
		λ	R	$\Re f_0$	$\Im f_0$	d_0
ΛK_S^0 & $\bar{\Lambda} K_S^0$	0-10%		2.96 ± 0.54 (stat.) ± 0.33 (sys.)			
	10-30%	0.60 ± 0.71 (stat.) ± 0.54 (sys.)	2.40 ± 0.45 (stat.) ± 0.29 (sys.)	-0.35 ± 0.10 (stat.) ± 0.21 (sys.)	0.19 ± 0.11 (stat.) ± 0.12 (sys.)	1.85 ± 0.61 (stat.) ± 2.68 (sys.)
	30-50%		1.77 ± 0.32 (stat.) ± 0.15 (sys.)			

Table 3: Fit Results $\Lambda(\bar{\Lambda})K_S^0$, with 10 residual correlations included. Each pair is fit simultaneously with its conjugate (ie. ΛK_S^0 with $\bar{\Lambda} K_S^0$) across all centralities (0-10%, 10-30%, 30-50%), for a total of 6 simultaneous analyses in the fit. A single λ parameter is shared amongst all. Each analysis has a unique normalization parameter. The radii are shared between analyses of like centrality, as these should have similar source sizes. The scattering parameters ($\Re f_0$, $\Im f_0$, d_0) are shared amongst all. The background is fit with a linear form in the range $0.6 < k^* < 0.9$ GeV/c. The fit is done on the data with only statistical error bars. The errors marked as “stat.” are those returned by MINUIT. The errors marked as “sys.” are those which result from my systematic analysis (as outlined in Section ??).

Fit Results $\Lambda(\bar{\Lambda})K^\pm$						
System	Centrality	Fit Parameters				
		λ	R	$\Re f_0$	$\Im f_0$	d_0
ΛK^+ & $\bar{\Lambda} K^-$	0-10%	1.87 ± 0.42 (stat.) ± 0.21 (sys.)	6.59 ± 0.80 (stat.) ± 0.49 (sys.)	-1.14 ± 0.17 (stat.) ± 0.31 (sys.)	0.66 ± 0.16 (stat.) ± 0.15 (sys.)	0.68 ± 0.46 (stat.) ± 0.53 (sys.)
	10-30%	1.27 ± 0.26 (stat.) ± 0.23 (sys.)	4.91 ± 0.53 (stat.) ± 0.28 (sys.)			
ΛK^+ & $\bar{\Lambda} K^-$	30-50%	1.07 ± 0.23 (stat.) ± 0.32 (sys.)	3.44 ± 0.36 (stat.) ± 0.13 (sys.)	0.52 ± 0.15 (stat.) ± 0.19 (sys.)	0.55 ± 0.10 (stat.) ± 0.18 (sys.)	-3.61 ± 1.20 (stat.) ± 1.02 (sys.)

Table 4: Fit Results $\Lambda(\bar{\Lambda})K^\pm$, with 10 residual correlations included. All ΛK^\pm analyses are fit simultaneously across all centralities (0-10%, 10-30%, 30-50%). Scattering parameters ($\Re f_0$, $\Im f_0$, d_0) are shared between pair-conjugate systems (i.e. a parameter set describing the ΛK^+ & $\bar{\Lambda} K^-$ system, and a separate set describing the ΛK^- & $\bar{\Lambda} K^+$ system). For each centrality, a radius and λ parameters are shared between all pairs (ΛK^+ , $\bar{\Lambda} K^-$, ΛK^- , $\bar{\Lambda} K^+$). Each analysis has a unique normalization parameter. The background is modeled by a (6th-)degree polynomial fit to THERMINATOR simulation. The fit is done on the data with only statistical error bars. The errors marked as “stat.” are those returned by MINUIT. The errors marked as “sys.” are those which result from my systematic analysis (as outlined in Section ??).

0.1.3 No Residual Correlations Included in Fit

Figure 16 nicely collects and summarizes all of our extracted fit parameters for the case of no included residual contributors. Figure 17 presents our extracted fit radii, along with those of other systems previously analyzed by ALICE [?], as a function of pair transverse mass (m_T). Figures 18, 19, and 20 show the experimental correlation functions with fits, assuming no residual contributors, for all studied centralities for ΛK_S^0 with $\bar{\Lambda} K_S^0$, ΛK^+ with $\bar{\Lambda} K^-$, and ΛK^- with $\bar{\Lambda} K^+$, respectively. The parameter sets extracted from the fits can be found in Tables 5 and 6.

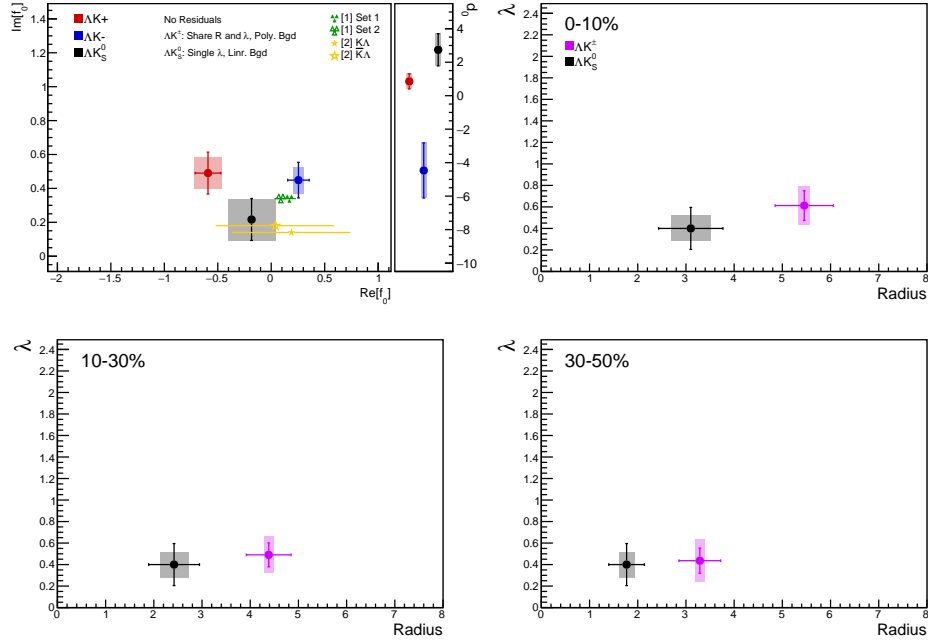


Fig. 16: Extracted scattering parameters for the case of NO residual contributors for all of our AK systems. [Top Left]: $\text{Im}f_0$ vs. $\text{Re}f_0$, together with d_0 to the right. [Top Right (Bottom Left, Bottom Right)]: λ vs. Radius for the 0-10% (10-30%, 30-50%) bin. The green [?] and yellow [?] points show theoretical predictions made using chiral perturbation theory.

Figure 17 shows extracted R_{inv} parameters as a function of transverse mass (m_T) for various pair systems over several centralities. The published ALICE data [?] is shown with transparent, open symbols. The new AK results are shown with opaque, filled symbols. The radii shown an increasing size with increasing centrality, as is expected from the simple geometric picture of the collisions. The radii decrease in size with increasing m_T , and we see an approximate scaling of the radii with transverse mass, as is expected in the presence of collective flow in the system.

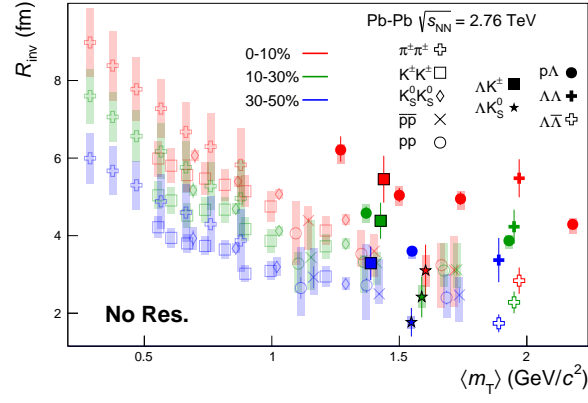
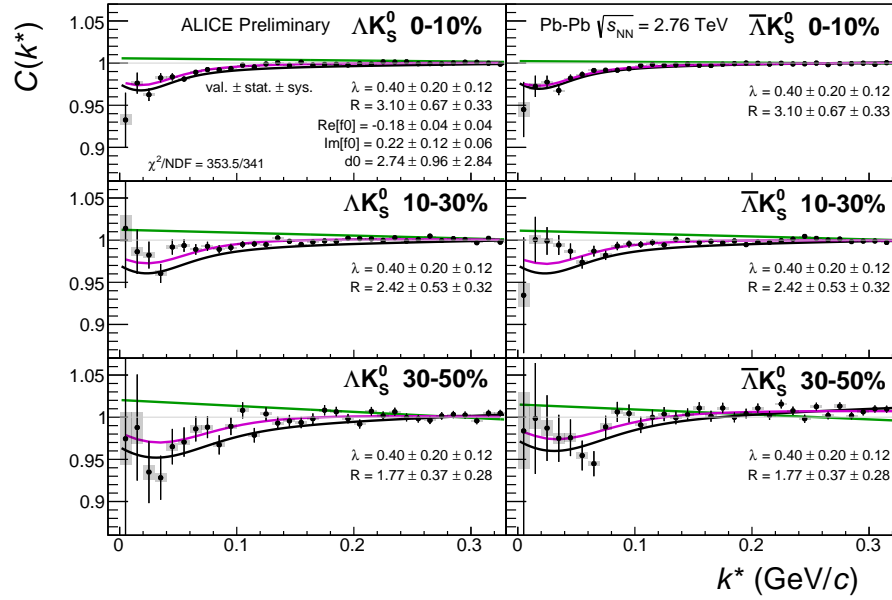
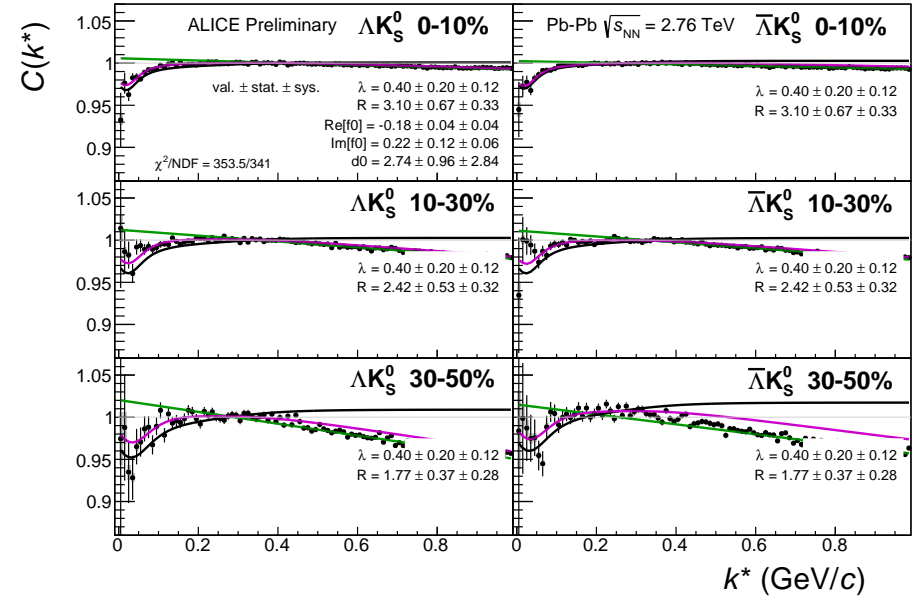


Fig. 17: No residual correlations in ΛK fits. Extracted fit R_{inv} parameters as a function of pair transverse mass (m_T) for various pair systems over several centralities. The ALICE published data [?] is shown with transparent, open symbols. The new ΛK results are shown with opaque, filled symbols. In the left, the ΛK^+ (with it's conjugate pair) results are shown separately from the ΛK^- (with it's conjugate pair) results. In the right, all ΛK^\pm results are averaged.

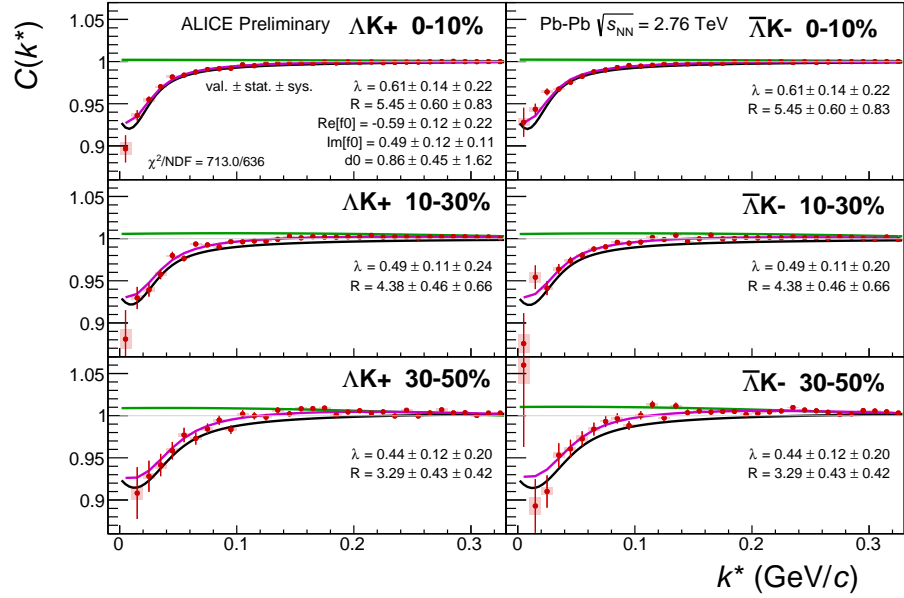


(a) Signal region view ($k^* \lesssim 0.3$ GeV/c)

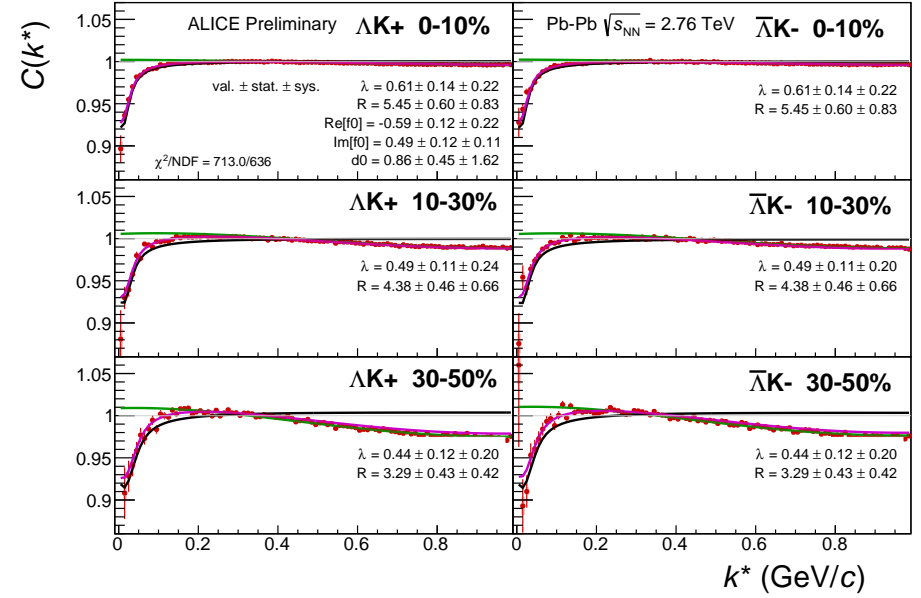


(b) Wide view ($k^* \lesssim 1.0$ GeV/c)

Fig. 18: Fits, with NO residual correlations included, to the ΛK_S^0 (left) and $\bar{\Lambda} K_S^0$ (right) data for the centralities 0-10% (top), 10-30% (middle), and 30-50% (bottom). The lines represent the statistical errors, while the boxes represent the systematic errors. A single λ parameter is shared amongst all. Each analysis has a unique normalization parameter. The radii are shared between analyses of like centrality, as these should have similar source sizes. The scattering parameters ($\text{Re}f_0$, $\text{Im}f_0$, d_0) are shared amongst all. The background is modeled by a (6th-)degree polynomial fit to THERMINATOR simulation. The black solid line represents the “raw” primary fit, i.e. not corrected for momentum resolution effects nor non-flat background. The green line shows the fit to the non-flat background. The purple points show the fit after momentum resolution and non-flat background corrections have been applied. The extracted fit values with uncertainties are printed.

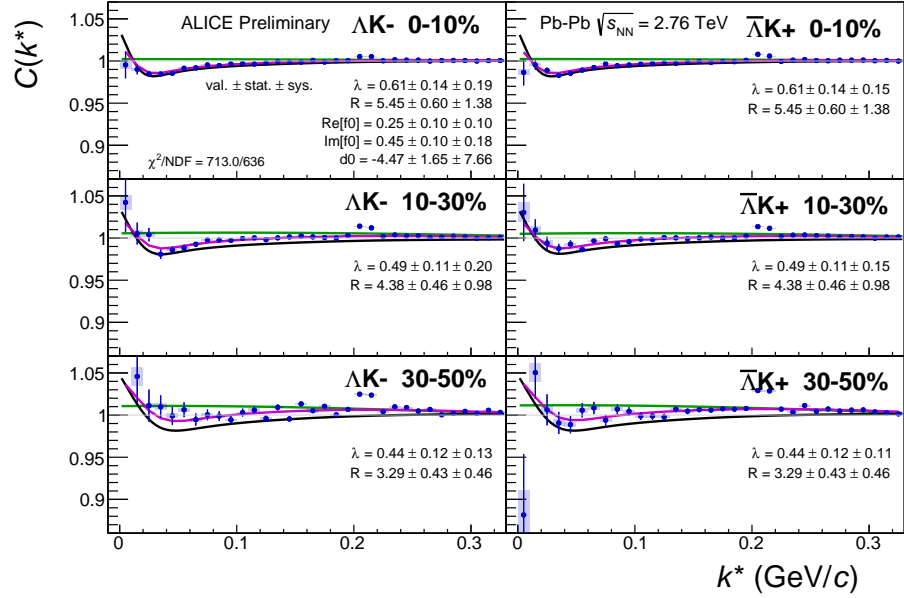


(a) Signal region view ($k^* \lesssim 0.3$ GeV/c)

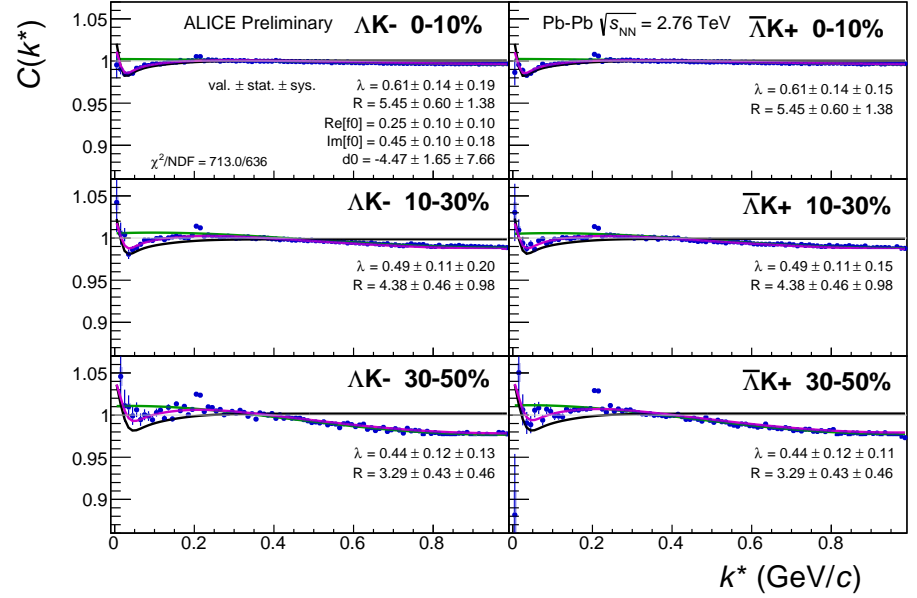


(b) Wide view ($k^* \lesssim 1.0$ GeV/c)

Fig. 19: Fits to the ΛK^+ (left) and $\bar{\Lambda} K^-$ (right) data for the centralities 0-10% (top), 10-30% (middle), and 30-50% (bottom). The lines represent the statistical errors, while the boxes represent the systematic errors. All ΛK^\pm analyses are fit simultaneously across all centralities (0-10%, 10-30%, 30-50%). Scattering parameters ($\text{Re}f_0$, $\text{Im}f_0$, d_0) are shared between pair-conjugate systems (i.e. a parameter set describing the ΛK^+ & $\bar{\Lambda} K^-$ system, and a separate set describing the ΛK^- & $\bar{\Lambda} K^+$ system). For each centrality, a radius and λ parameters are shared between all pairs (ΛK^+ , $\bar{\Lambda} K^-$, ΛK^- , $\bar{\Lambda} K^+$). Each analysis has a unique normalization parameter. The background is modeled by a (6th-)degree polynomial fit to THERMINATOR simulation. The black solid line represents the “raw” primary fit, i.e. not corrected for momentum resolution effects nor non-flat background. The green line shows the fit to the non-flat background. The purple points show the fit after momentum resolution and non-flat background corrections have been applied. The extracted fit values with uncertainties are printed.



(a) Signal region view ($k^* \lesssim 0.3$ GeV/c)



(b) Wide view ($k^* \lesssim 1.0$ GeV/c)

Fig. 20: Fits, with NO residual correlations included, to the ΛK^- (left) with $\bar{\Lambda} K^+$ (right) data for the centralities 0-10% (top), 10-30% (middle), and 30-50% (bottom). The lines represent the statistical errors, while the boxes represent the systematic errors. All ΛK^\pm analyses are fit simultaneously across all centralities (0-10%, 10-30%, 30-50%). Scattering parameters ($\text{Re}f_0$, $\text{Im}f_0$, d_0) are shared between pair-conjugate systems (i.e. a parameter set describing the ΛK^+ & $\bar{\Lambda} K^-$ system, and a separate set describing the ΛK^- & $\bar{\Lambda} K^+$ system). For each centrality, a radius and λ parameters are shared between all pairs (ΛK^+ , $\bar{\Lambda} K^-$, ΛK^- , $\bar{\Lambda} K^+$). Each analysis has a unique normalization parameter. The background is modeled by a (6th-)degree polynomial fit to THERMINATOR simulation. The black solid line represents the “raw” primary fit, i.e. not corrected for momentum resolution effects nor non-flat background. The green line shows the fit to the non-flat background. The purple points show the fit after momentum resolution and non-flat background corrections have been applied. The extracted fit values with uncertainties are printed.

Fit Results $\Lambda(\bar{\Lambda})K_S^0$						
System	Centrality	Fit Parameters				
		λ	R	$\Re f_0$	$\Im f_0$	d_0
ΛK_S^0 & $\bar{\Lambda} K_S^0$	0-10%		3.10 ± 0.67 (stat.) ± 0.41 (sys.)			
	10-30%	0.40 ± 0.20 (stat.) ± 0.12 (sys.)	2.42 ± 0.53 (stat.) ± 0.29 (sys.)	-0.18 ± 0.04 (stat.) ± 0.22 (sys.)	0.22 ± 0.12 (stat.) ± 0.12 (sys.)	2.74 ± 0.96 (stat.) ± 1.28 (sys.)
	30-50%		1.77 ± 0.37 (stat.) ± 0.16 (sys.)			

Table 5: Fit Results $\Lambda(\bar{\Lambda})K_S^0$, with no residual correlations included. Each pair is fit simultaneously with its conjugate (ie. ΛK_S^0 with $\bar{\Lambda} K_S^0$) across all centralities (0-10%, 10-30%, 30-50%), for a total of 6 simultaneous analyses in the fit. A single λ parameter is shared amongst all. Each analysis has a unique normalization parameter. The radii are shared between analyses of like centrality, as these should have similar source sizes. The scattering parameters ($\Re f_0$, $\Im f_0$, d_0) are shared amongst all. The background is fit with a linear form in the range $0.6 < k^* < 0.9$ GeV/c. The fit is done on the data with only statistical error bars. The errors marked as “stat.” are those returned by MINUIT. The errors marked as “sys.” are those which result from my systematic analysis (as outlined in Section ??).

Fit Results $\Lambda(\bar{\Lambda})K^\pm$						
System	Centrality	Fit Parameters				
		λ	R	$\Re f_0$	$\Im f_0$	d_0
ΛK^+ & $\bar{\Lambda} K^-$	0-10%	0.61 ± 0.14 (stat.) ± 0.18 (sys.)	5.45 ± 0.60 (stat.) ± 0.12 (sys.)	-0.59 ± 0.12 (stat.) ± 0.13 (sys.)	0.49 ± 0.12 (stat.) ± 0.09 (sys.)	0.86 ± 0.45 (stat.) ± 1.63 (sys.)
	10-30%	0.49 ± 0.11 (stat.) ± 0.17 (sys.)	4.38 ± 0.46 (stat.) ± 0.10 (sys.)			
ΛK^+ & $\bar{\Lambda} K^-$	30-50%	0.44 ± 0.12 (stat.) ± 0.20 (sys.)	3.29 ± 0.43 (stat.) ± 0.10 (sys.)	0.25 ± 0.10 (stat.) ± 0.05 (sys.)	0.45 ± 0.10 (stat.) ± 0.08 (sys.)	-4.47 ± 1.65 (stat.) ± 1.60 (sys.)

Table 6: Fit Results $\Lambda(\bar{\Lambda})K^\pm$, with no residual correlations included. All ΛK^\pm analyses are fit simultaneously across all centralities (0-10%, 10-30%, 30-50%). Scattering parameters ($\Re f_0$, $\Im f_0$, d_0) are shared between pair-conjugate systems (i.e. a parameter set describing the ΛK^+ & $\bar{\Lambda} K^-$ system, and a separate set describing the ΛK^- & $\bar{\Lambda} K^+$ system). For each centrality, a radius and λ parameters are shared between all pairs (ΛK^+ , $\bar{\Lambda} K^-$, ΛK^- , $\bar{\Lambda} K^+$). Each analysis has a unique normalization parameter. The background is modeled by a (6th-)degree polynomial fit to THERMINATOR simulation. The fit is done on the data with only statistical error bars. The errors marked as “stat.” are those returned by MINUIT. The errors marked as “sys.” are those which result from my systematic analysis (as outlined in Section ??).

0.1.4 Fit Method Comparisons

In Figure 21, we show extracted fit parameters for the case of $\Lambda K^+(\bar{\Lambda} K^-)$ sharing radii with $\Lambda K^-(\bar{\Lambda} K^+)$. The figure shows results for three different treatments of the non-femtoscopic background: a polynomial fit to THERMINATOR 2 simulation to model the background (circles), a linear fit to the data to model the background (squares), and the Stavinsky method (crosses). The green [?] and yellow [?] points show theoretical predictions made using chiral perturbation theory.

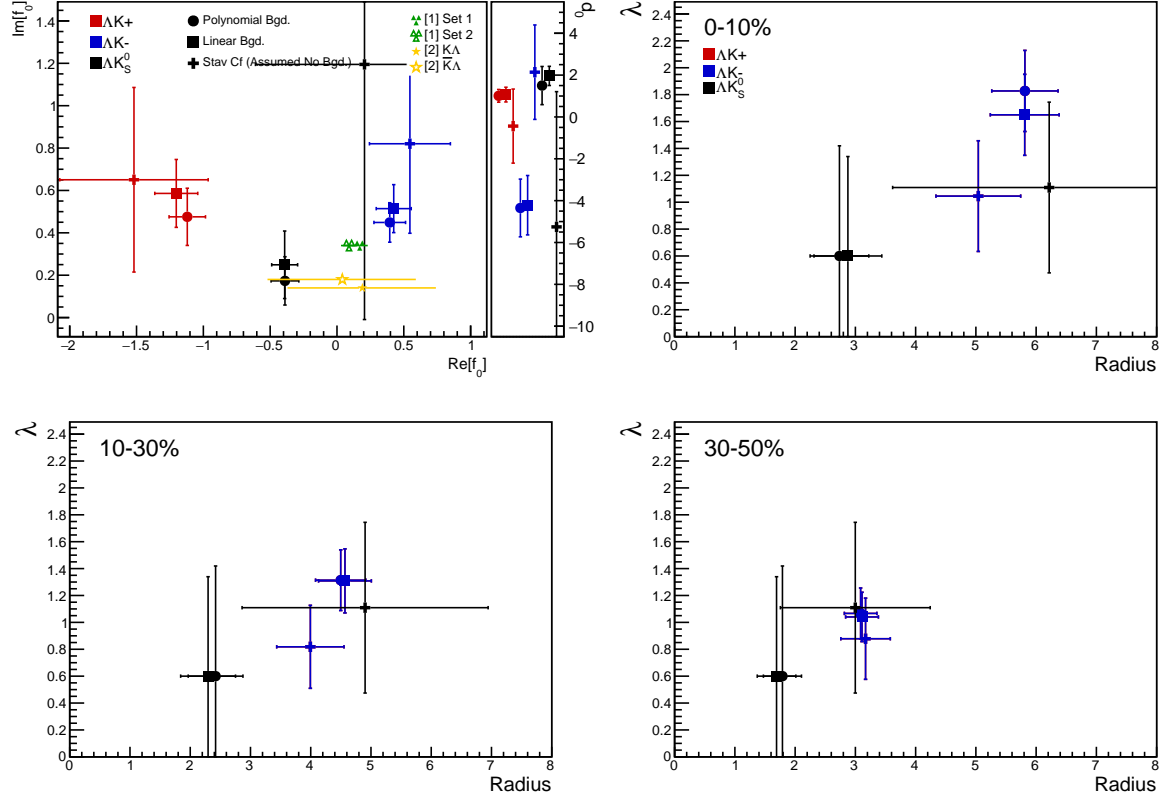


Fig. 21: Compare Fit Parameters: Background treatment: Extracted fit results for all of our $\Lambda(\bar{\Lambda})K^\pm$ systems across all studied centrality bins (0-10%, 10-30%, 30-50%). The $\Lambda K^+(\bar{\Lambda} K^-)$ and $\Lambda K^-(\bar{\Lambda} K^+)$ systems share both a radius and a λ parameter for each centrality bin (i.e. 3 total radius parameters, 3 total λ parameters). The figure shows results for three different treatments of the non-femtoscopic background: a polynomial fit to THERMINATOR 2 simulation to model the background (circles), a linear fit to the data to model the background (squares), and the Stavinsky method (crosses). The green [?] and yellow [?] points show theoretical predictions made using chiral perturbation theory.

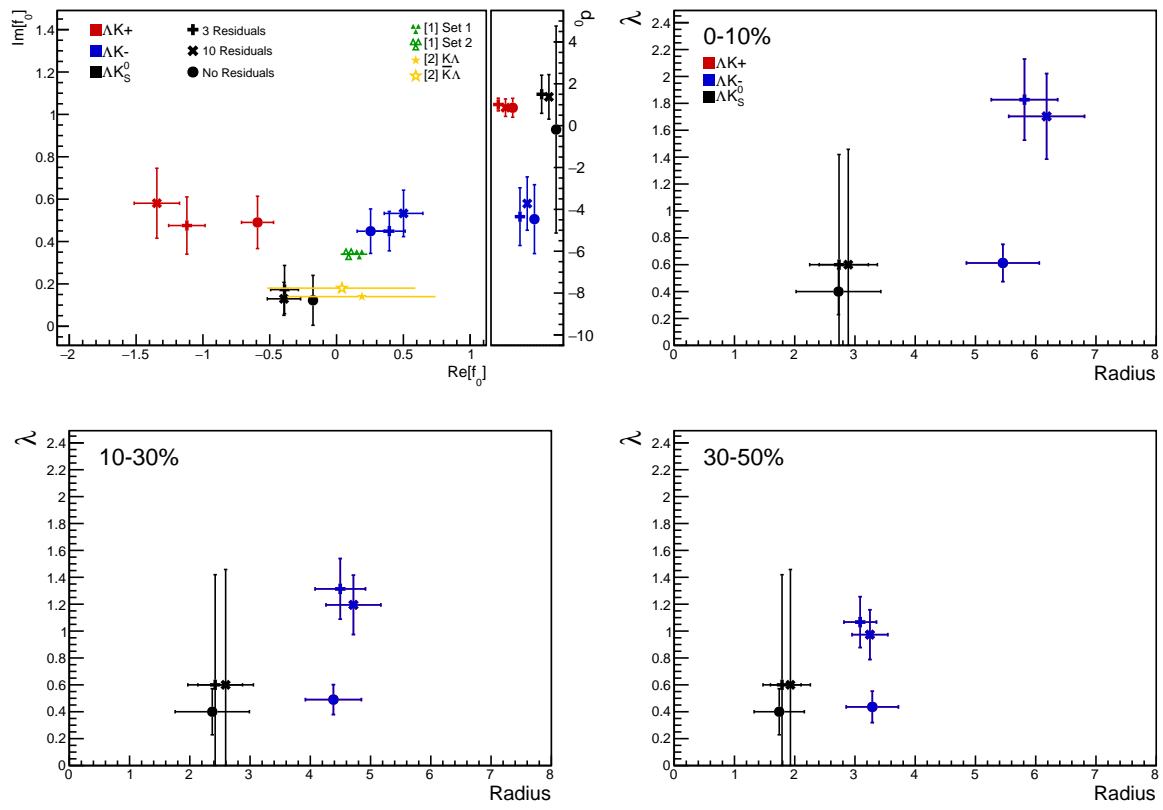


Fig. 22: Compare Fit Parameters: Number of residuals: Results shown for the case of 3 (+), 10 (X), and no (circles) residual contributors.

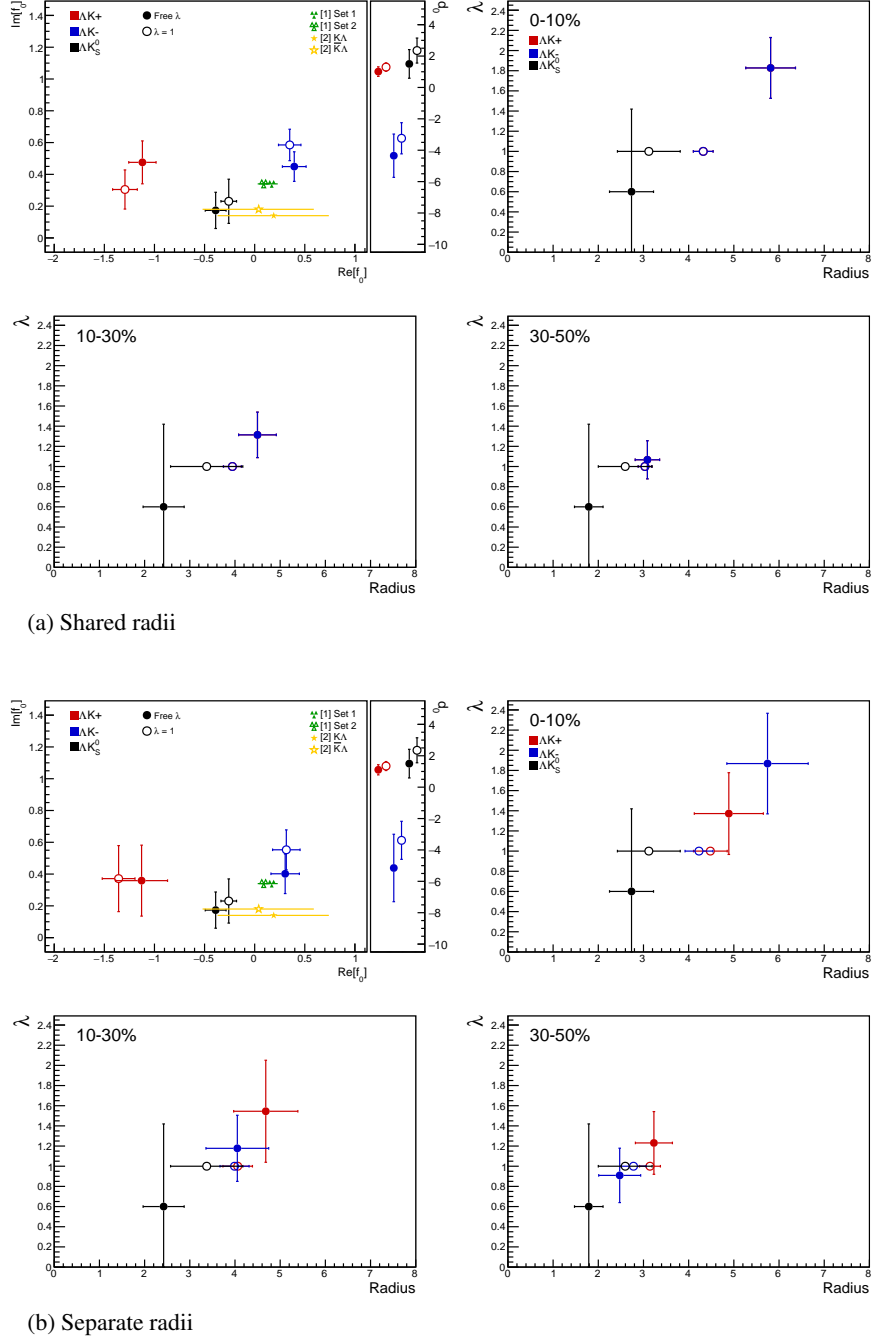
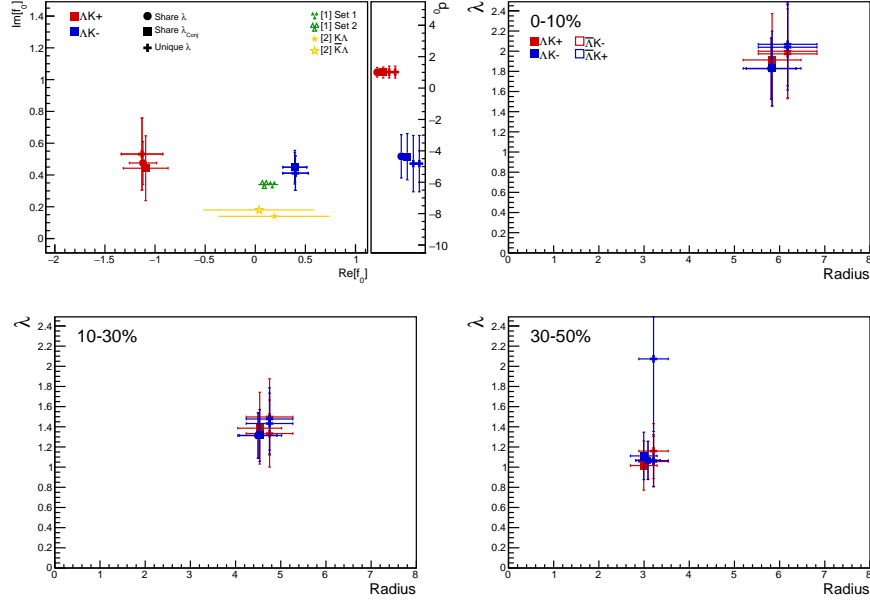
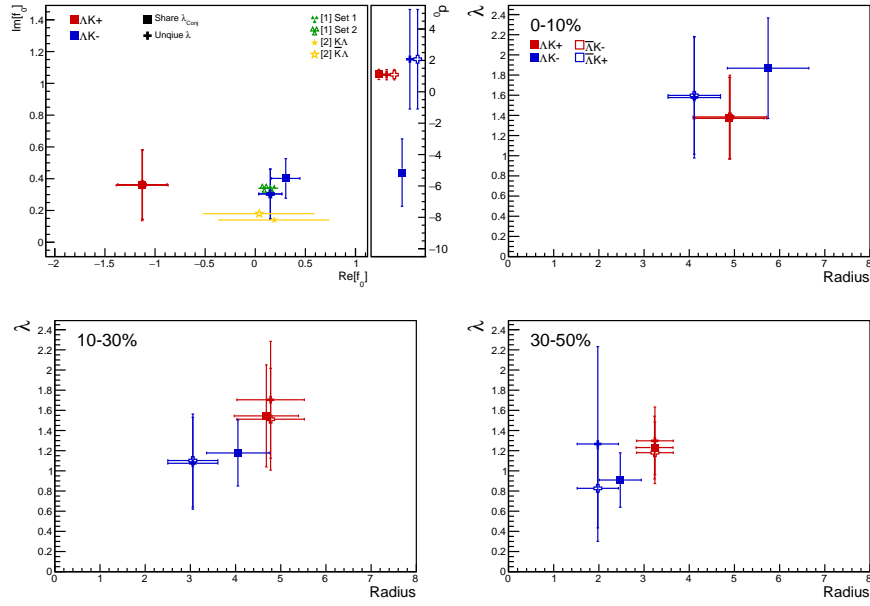


Fig. 23: Compare Fit Parameters: Free vs fixed λ : Results shown for λ parameters left free (filled symbols) and fixed to 1 (open symbols). In the top plot (23a), the ΛK^+ and ΛK^- analyses share radii, whereas in the bottom (23b) they have unique radii.



(a) Shared radii



(b) Separate radii

Fig. 24: Compare Fit Parameters: Shared vs unique λ : Results shown for different sharing of the λ parameters between analyses and systems. In the top (24a), the ΛK^+ and ΛK^- analyses share radii, whereas in the bottom (24b), they do not. “Share λ ” (circles) is the case where a single λ is shared amongst all analyses for a given centrality bin (i.e., in 24a, 3 radius parameters and 3 λ parameters). “Share λ_{conj} ” (squares) means that conjugate pairs (ex. ΛK^+ and $\bar{\Lambda} K^-$) share a λ parameter for each centrality. This corresponds to 6 total λ parameters (for each of the 3 centrality bins, the ΛK^+ ($\bar{\Lambda} K^-$) receives a unique λ , as does ΛK^- ($\bar{\Lambda} K^+$)). Finally, in “Unique λ ” (+), each analysis received its own unique λ parameter. This corresponds to 12 λ parameters (for each of the 3 centrality bins, each ΛK^+ , $\bar{\Lambda} K^-$, ΛK^- , and $\bar{\Lambda} K^+$ receives a unique λ).

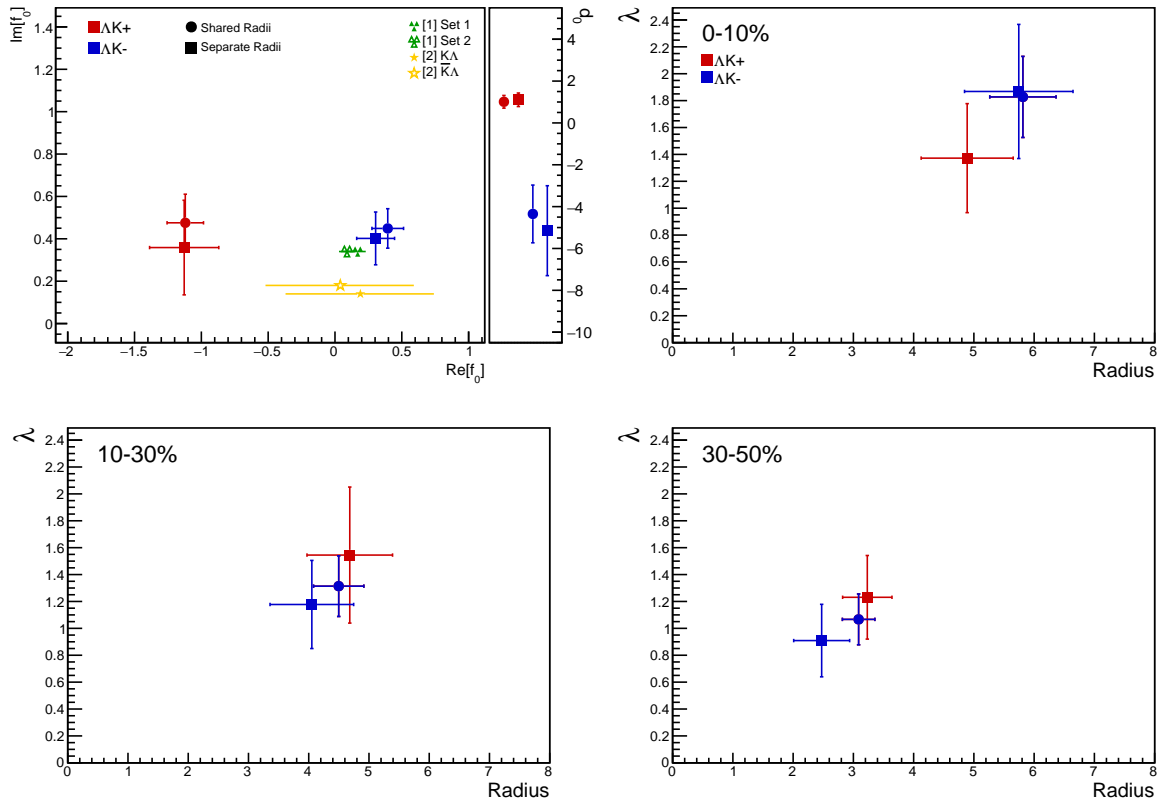


Fig. 25: Compare Fit Parameters: Shared vs. Separate Radii: Results shown for the case of radii being shared between $\Lambda K^+(\bar{\Lambda} K^-)$ and $\Lambda K^-(\bar{\Lambda} K^+)$ (circles) vs not shared (squares).

0.1.5 Discussion of m_T -Scaling

Discuss why m_T scaling is not appropriate for non-identical femtoscopy studies.